Supporting Information

A core-shell liquid metal-Cu nanoparticle with GSH consumption via in-situ replacement strategy for tumor combination treatment of chemodynamic, microwave dynamic and microwave thermal therapy

Yongnian Yu[ab], Qiong Wu[b], Meng Niu[c], Li Gou*[a], Longfei Tan*[b], Changhui Fu[b], Xiangling Ren[b], Jun Ren[b], Yongfa Zheng[*d],and Xianwei Meng*[b]

[a] College of Biomedical Engineering, Sichuan University, Chengdu 610065, China.

[b] Laboratory of Controllable Preparation and Application of Nanomaterials, Technical Institute of Physics and Chemistry, Chinese Academy of Sciences, Beijing 100190, China. CAS Key Laboratory of Cryogenics, Technical Institute of Physics and Chemistry, Beijing 100190, China.

[c] Department of Radiology, First Hospital of China Medical University, Shenyang 110001, China

[d] Department of Oncology, Renmin Hospital of Wuhan University, Wuhan 430060, China

Tab. S1 Elements contents of LZC@IL

element	wt.%	at.%
O K	4.79	18.63
Cu K	35.21	34.46
Ga K	39.68	35.39
Zr K	3.72	2.53
In L	16.60	8.99

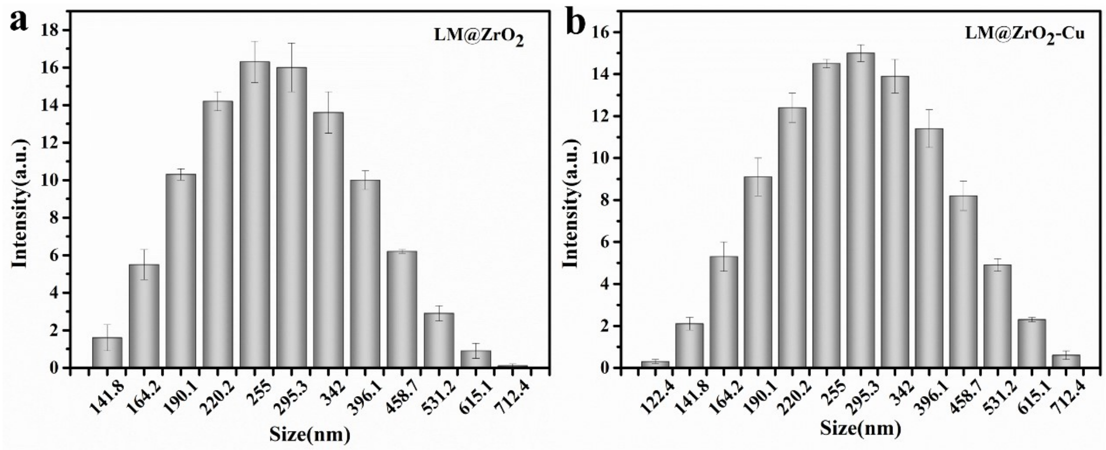

Fig. S1. Hydrodynamic size of LZ and LZC.

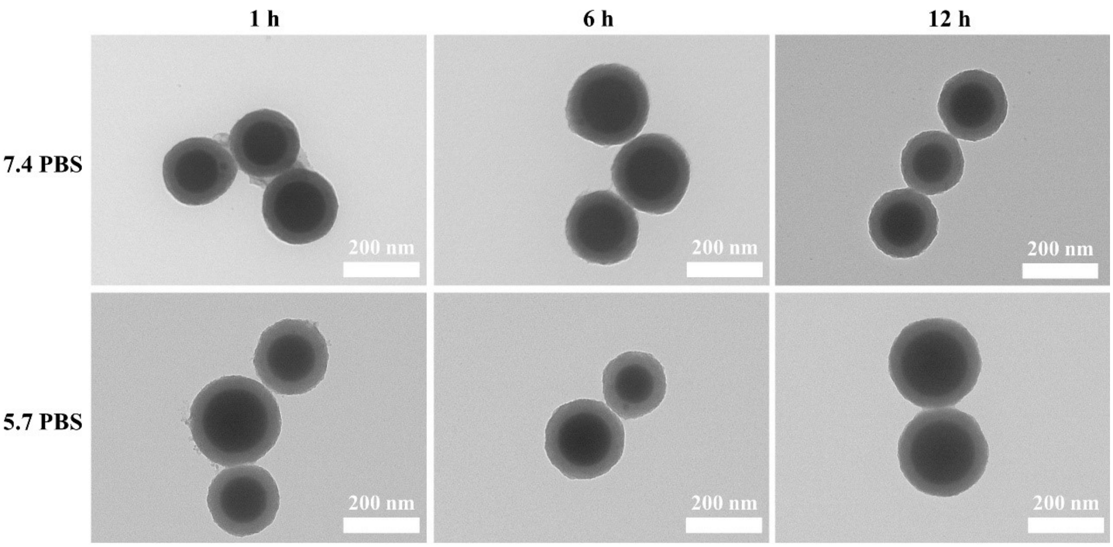

Fig. S2. TEM of LZC in PBS of different pH at 1, 6, 12 h.

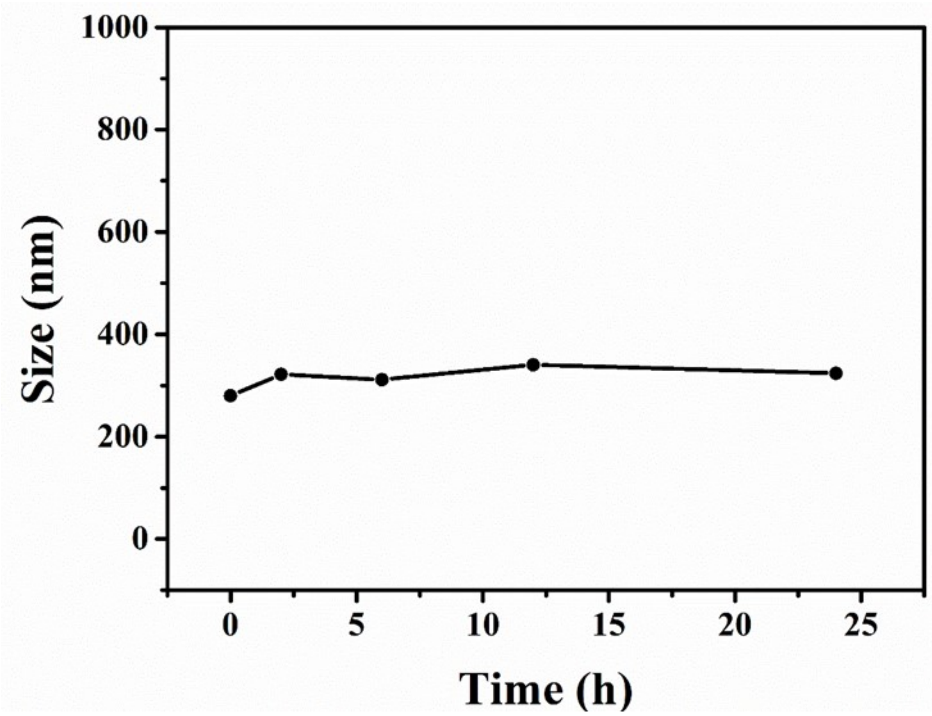

Fig. S3. Hydrodynamic size of the particles of LZC in 7.4 PBS at 2, 6, 12, 24 h.

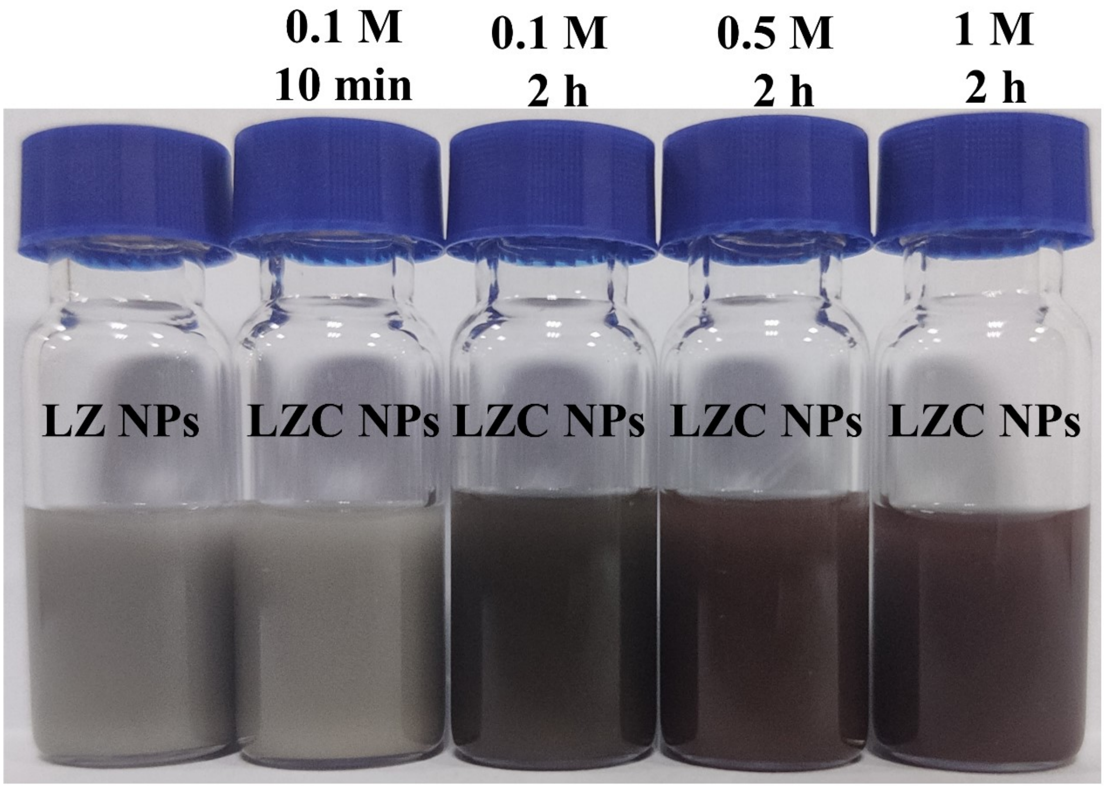

Fig. S4. Photographs of different product.

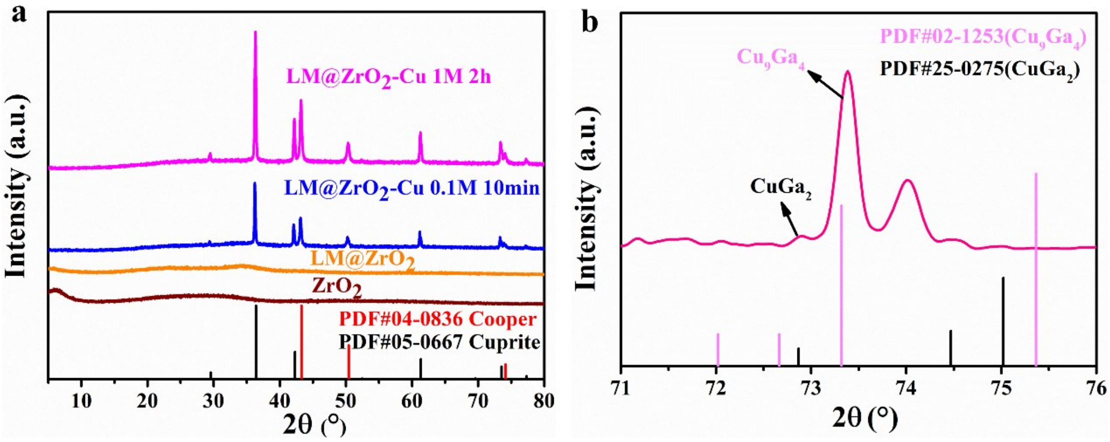

Fig. S5. XRD spectra of different materials and standard PDF card of cooper, cuprite, $CuGa_2$ and Cu_9Ga_4.

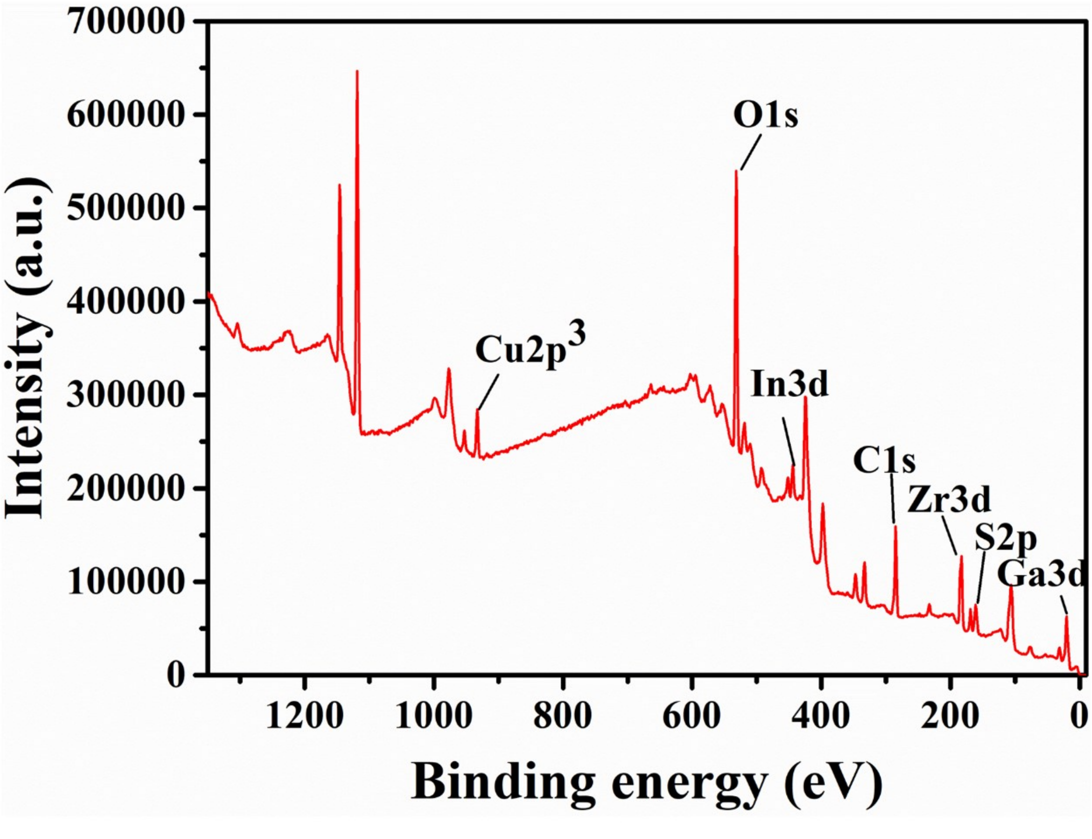

Fig. S6. XPS spectra of LZC.

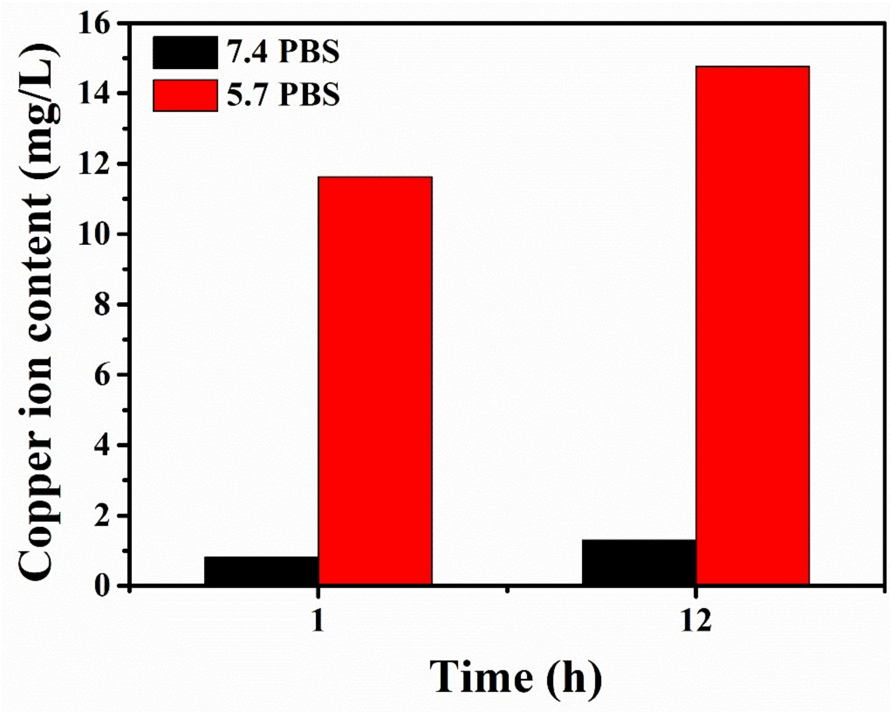

Fig. S7. The release of cooper ion under different pH conditions.

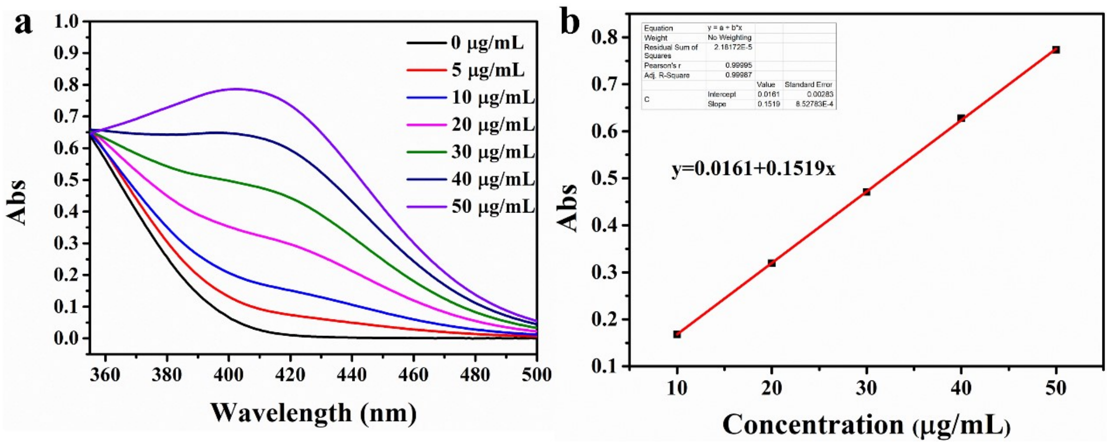

Fig. S8. The absorption of GSH of different concentration (a) and standard content curve of GSH (b).

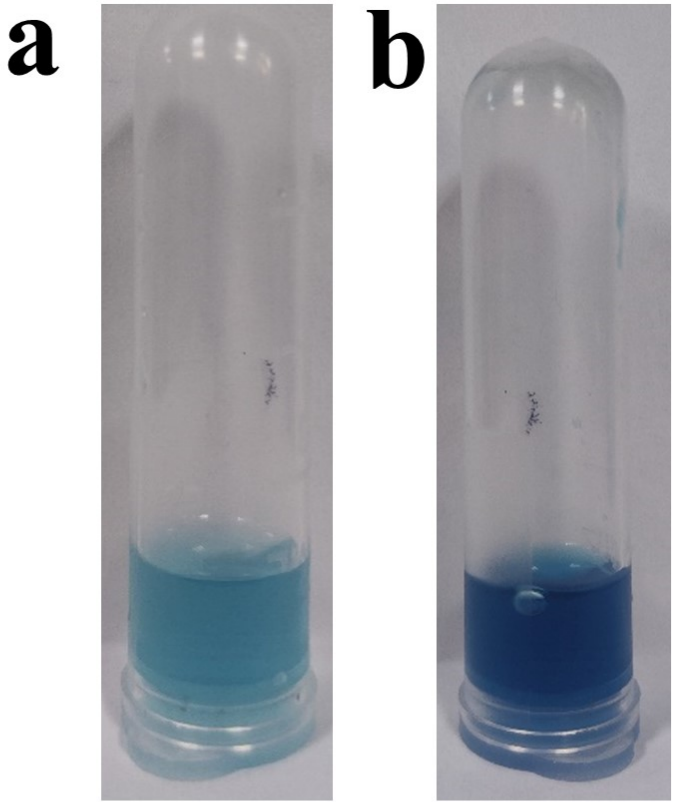

Fig. S9. The generation of Cu^{+} under GSH treatment. a) 15 min. b) 1 h.

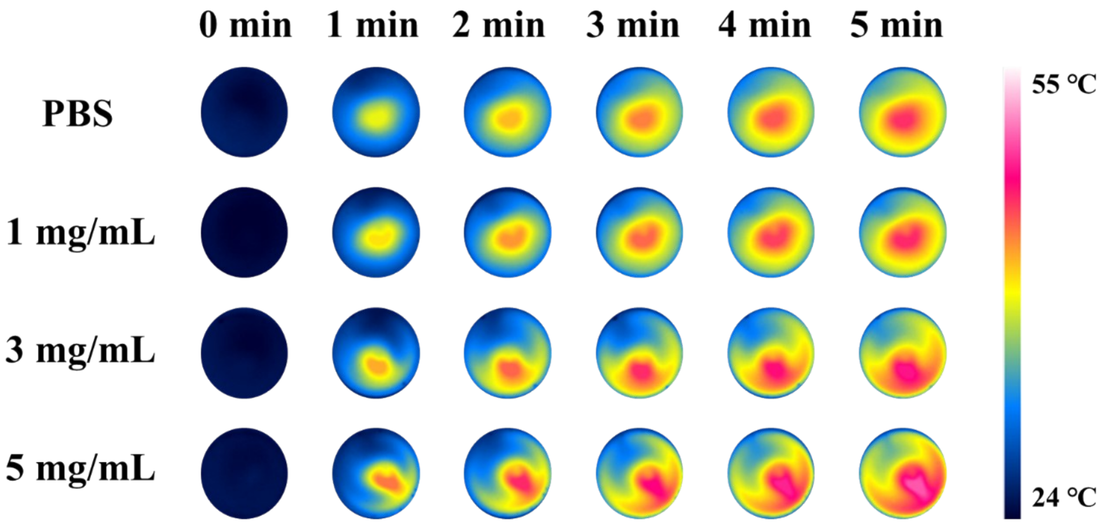

Fig. S10. The infrared thermal image of LZC of different concentration within 5 min.

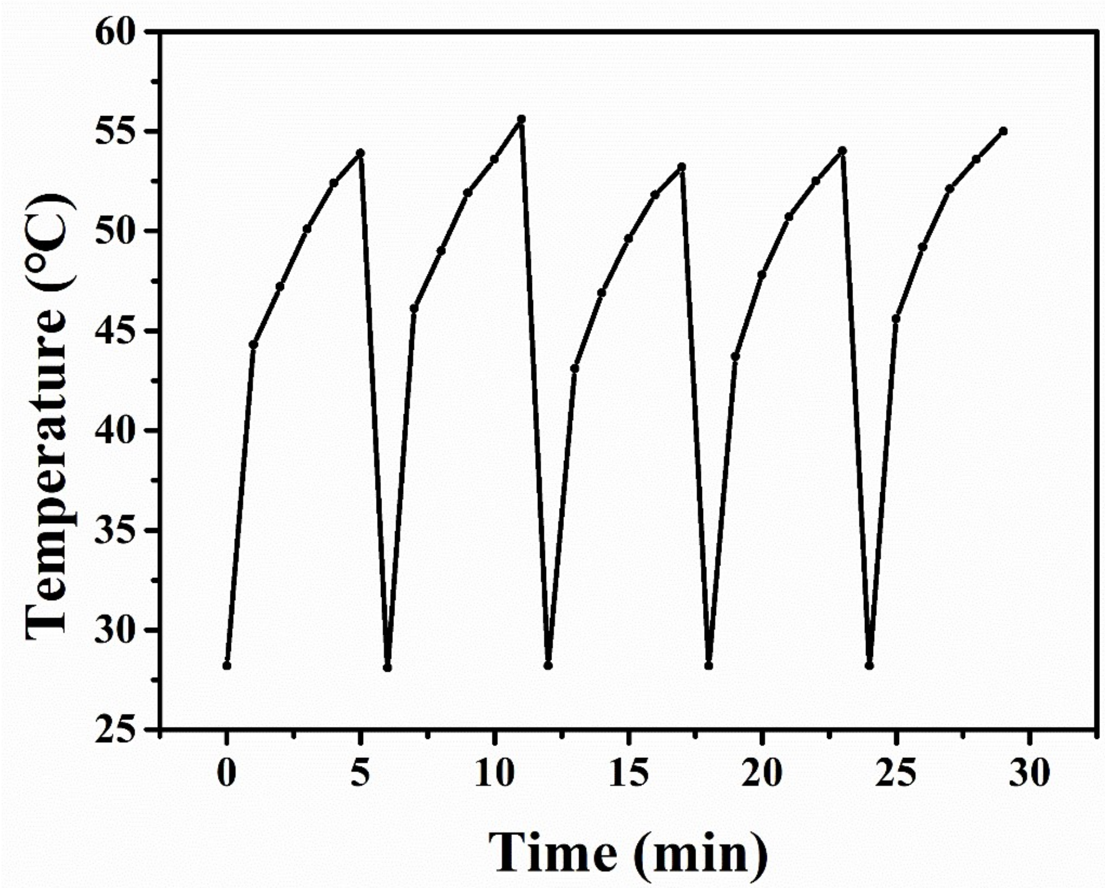

Fig. S11. The microwave thermal stability of LZC@IL.

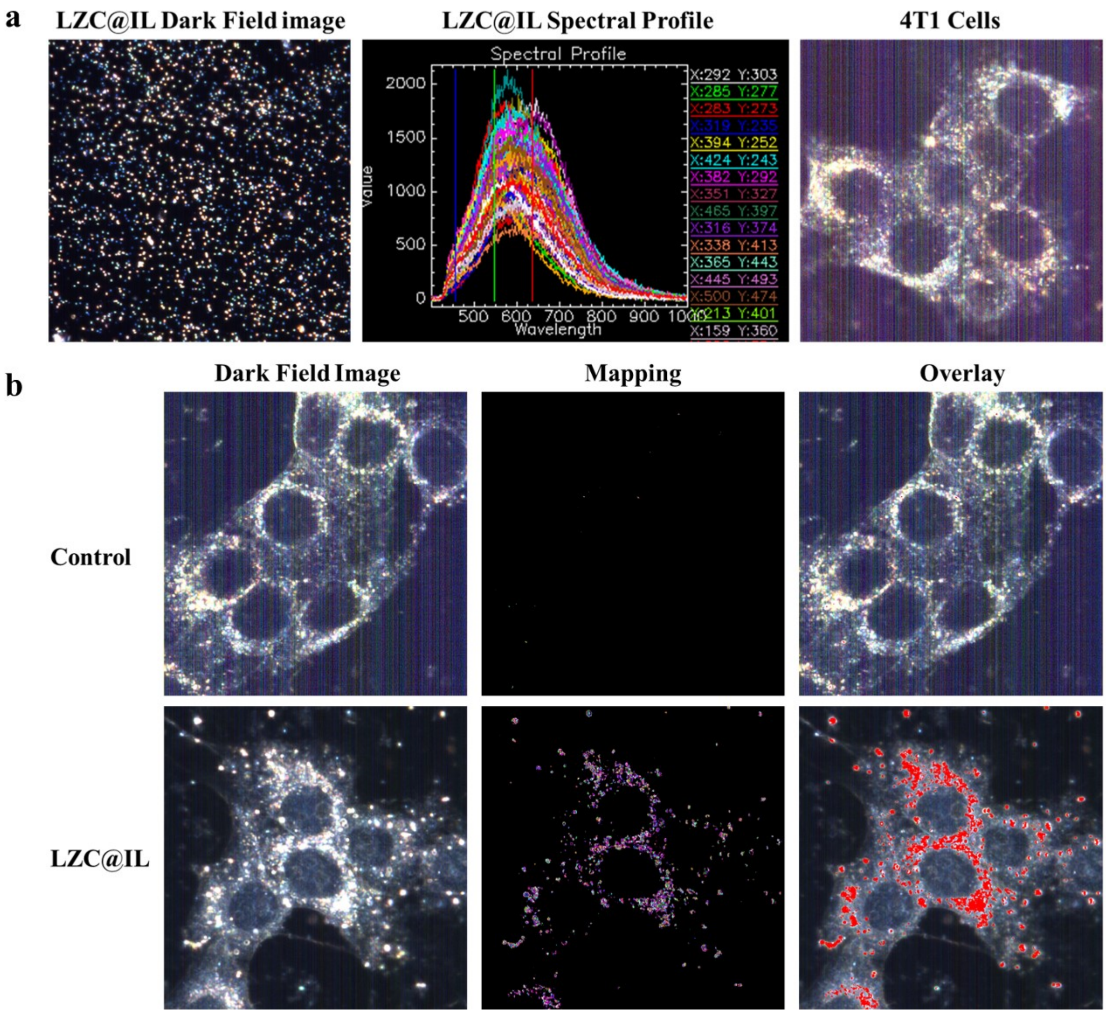

Fig. S12. Cellular uptake study by hyperspectral. a) the dark field image of LZC@IL and the image of 4T1 cells. b) The mapping image of cell and LZC@IL.

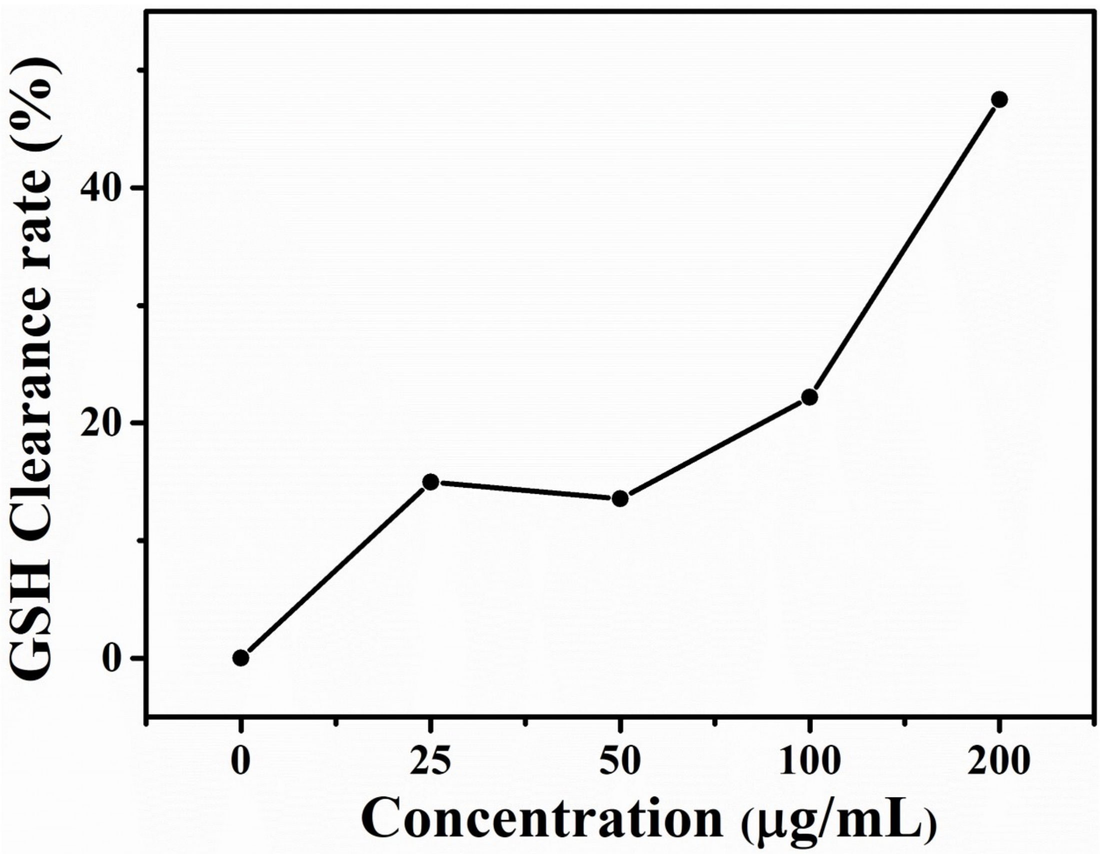

Fig. S13. Cellular GSH clearance rate of different concentration of LZC.

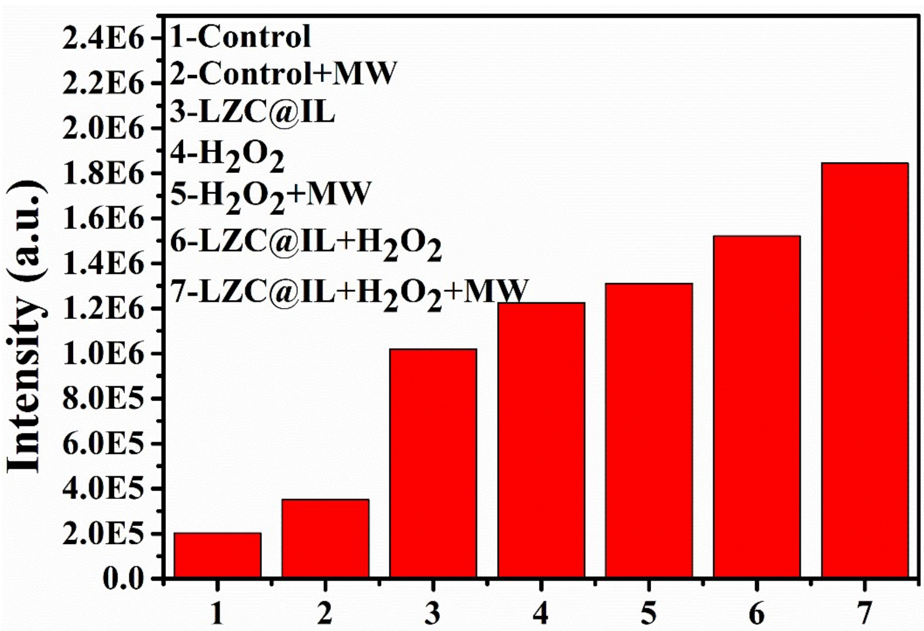

Fig. S14. The mean FL intensity of DCF of each group measured by ImageJ.

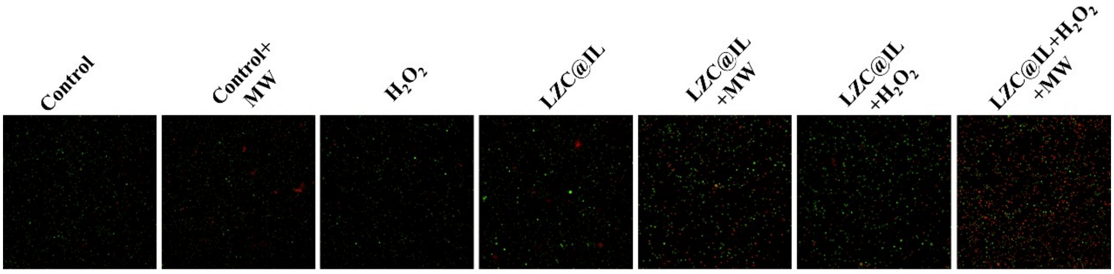

Fig. S15. The live/dead staining assay (scale bar: 200 μm).

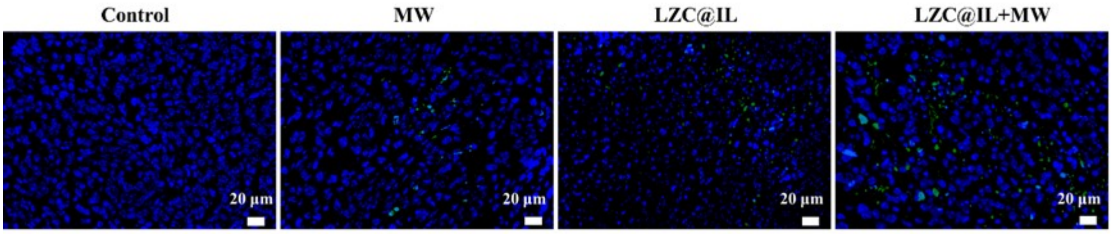

Fig. S16. TUNEL staining of tumor sections after different treatments.